

SCIENTIFIC REPORTS



OPEN

Fasting and Feeding Signals Control the Oscillatory Expression of *Angptl8* to Modulate Lipid Metabolism

Received: 10 August 2016
Accepted: 24 October 2016
Published: 15 November 2016

Fabin Dang¹, Rong Wu¹, Pengfei Wang¹, Yuting Wu¹, Md. Shofiu Azam¹, Qian Xu²,
Yaqiong Chen¹ & Yi Liu¹

Emerging evidence implies a key role of angiotensin-like protein 8 (*Angptl8*) in the metabolic transition between fasting and feeding, whereas much less is known about the mechanism of its own expression. Here we show that hepatic *Angptl8* is rhythmically expressed, which involving the liver X receptor alpha (LXR α) and glucocorticoid receptor (GR) modulation during feeding and fasting periods, respectively. In addition, *Angptl8* mRNA is very unstable, which contributes to the nature of its daily rhythmicity by rapidly responding to fasting/feeding transition. To explore its pathological function in dexamethasone (DEX)-induced fatty liver, we reversed its suppression by glucocorticoids through adenoviral delivery of *Angptl8* gene in mouse liver. Surprisingly, hepatic overexpression of *Angptl8* dramatically elevated plasma triglyceride (TG) and non-esterified fatty acid (NEFA) levels in DEX-treated mice, suggesting a metabolic interaction between *Angptl8* and glucocorticoid signaling. Moreover, intracellular hepatic *Angptl8* is implicated in the regulation of lipid homeostasis by the experiments with ectopic expression of a nonsecreted *Angptl8* mutant (Δ 25-*Angptl8*). Altogether, our data demonstrate the molecular mechanism of the diurnal rhythm of *Angptl8* expression regulated by glucocorticoid signaling and LXR α pathway, and provide new evidence to understand the role of *Angptl8* in maintaining plasma TG homeostasis.

Hypertriglyceridemia is one of major risk factors of nonalcoholic fatty liver (NAFL), and elevated serum triglycerides (TG) commonly associates with insulin resistance and represent a valuable clinical marker of the metabolic syndrome^{1,2}. Plasma TG concentrations are mainly determined by the balance between their production and clearance. The former involves the synthesis of very low density lipoprotein triglyceride (VLDL-TG) and chylomicron triglyceride (chylomicron-TG) in the liver and small intestine^{3,4}, respectively, while the latter involves lipoprotein lipase (LPL)-mediated lipolysis of VLDL-TG⁵.

Angiotensin-like proteins (Angptls) are a family of proteins structurally similar to the angiotensins. Angptls have emerged as crucial regulators of circulating TG levels and thus have been expected as potential targets for metabolic syndrome therapy in recent years^{6,7}. For instance, *Angptl3* and *Angptl4* have been reported to inhibit LPL activity to impair TG clearance^{8–10}. Several studies with *Angptl8*-deficient and/or *Angptl8*-overexpressing mice have revealed that *Angptl8*, similar to *Angptl3* and 4, plays an important role in modulating circulating TG clearance via the inhibition of LPL activity^{11–13}. Of note, overexpression of *Angptl3* alone does not alter the levels of circulating TG, whereas co-expressing it with *Angptl8* results in hypertriglyceridemia in mice¹¹. On the other hand, ectopic expression of *Angptl8* in *Angptl3*-null mice has also little effect on plasma TG levels¹¹. These results indicate that *Angptl3* and *Angptl8* have to function together *in vivo*.

Previous studies have shown that *Angptl8* is dramatically suppressed by fasting and significantly induced by refeeding in mice^{12,14,15}. Although many efforts have been taken^{12,15–17}, the regulatory mechanisms of *Angptl8* gene expression remain inconclusive. Here we show that the liver X receptor alpha (LXR α) and glucocorticoid receptor

¹Key Laboratory of Nutrition and Metabolism, Institute for Nutritional Sciences, Shanghai Institutes for Biological Sciences, University of Chinese Academy of Sciences, Chinese Academy of Sciences, 320 Yueyang Road Shanghai, 200031, China. ²Department of Endocrinology, The First Affiliated Hospital of Harbin Medical University, No. 23 Youzheng Street, NanGang District, Harbin, 150001, China. Correspondence and requests for materials should be addressed to Y.L. (email: liuyi@sibs.ac.cn)

(GR) are involved in mediating the induction and suppression of *Angptl8* expression in mouse liver during feeding and fasting periods, respectively, which combines with the very short half-life of *Angptl8* mRNA to result in the circadian pattern of its expression. Additionally, results from the experiments of overexpressing *Angptl8* in mouse liver suggest that *Angptl8* affects hepatic expression of genes involved in non-esterified fatty acid (NEFA) uptake, TG mobilization and VLDL secretion, as well as promoting lipolysis in adipose tissue in the context of dexamethasone (DEX) injection, suggesting a tightly metabolic interaction between *Angptl8* and glucocorticoid signaling.

Results

Hepatic *Angptl8* expression oscillates in a peripheral clock-independent manner. As plasma TG levels oscillate rhythmically in a 24-hour cycle¹⁸, and *Angptl8* plays an important role in maintaining lipid metabolism^{11,13,19}, we speculated that *Angptl8* expression may also exhibit circadian pattern. Thus, we checked the temporal expression of *Angptl8* in livers from mice euthanized at every 4-hour intervals throughout the day. Indeed, hepatic expression of *Angptl8* gene oscillated rhythmically with plateau near ZT16 and nadir around ZT4 (Fig. 1a,b). Considering that *Bmal1*, which serves as a core component of the circadian clock to govern the rhythmic expression of many genes²⁰, is involved in regulating lipid homeostasis²¹, we wondered whether the circadian expression of *Angptl8* is controlled by *Bmal1*. To answer this question, we then examined the expression pattern of hepatic *Angptl8* in liver-specific *Bmal1*-knockout (*L-Bmal1*^{-/-}) mice. Unexpectedly, the rhythmic expression of *Angptl8* was almost unaffected by *Bmal1* deficiency (Fig. 1c). Consistently, *Angptl8* protein profiles in the liver and plasma were nearly identical between *L-Bmal1*^{-/-} mice and its wild-type littermates (Fig. 1d). Together, these results suggest that the expression of *Angptl8* oscillates diurnally in the liver, which is not controlled by hepatic core clock.

Fasting and feeding signals modulate the expression of *Angptl8*. Since the expression of *Angptl8* is tightly associated with nutritional status^{12,14,15}, we then performed food entrainment experiments to explore whether food availability is a potential synchronizer for *Angptl8* oscillation. As expected, daytime-restricted feeding (DF) completely reversed the phase of mRNA and protein accumulations of *Angptl8* in the liver, as well as its secretion pattern, compared to those with nighttime-feeding (NF, Fig. 1e,f). We further investigated the involvement of feeding style in synchronizing *Angptl8* expression by euthanizing mice at 4-hour intervals around the clock during 28-hour fasting initiated from Day1-ZT12 to Day2-ZT16 and 2-hour intervals after refeeding from Day2-ZT12 to Day2-ZT16. Compared to those in ad libitum-fed mice, the diurnal oscillations of *Angptl8* mRNA and *Angptl8* protein accumulations were strikingly abolished by fasting, whereas were recovered by refeeding (Fig. 1g,h). Taken together, these data favor the conclusion that fasting and feeding signals play critical roles in generating the circadian oscillation of *Angptl8* expression.

LXR α upregulates hepatic *Angptl8* expression in refed mice. *Angptl8*, also named as RIFL (refeeding induced fat and liver)¹⁵, has been reported to be an insulin target gene and upregulated in HepG2 cells by the treatment of T0901317¹⁷, a ligand of liver X receptor α (LXR α) that regulates lipid metabolic gene expression in response to insulin. Indeed, we found that T0901317 promoted *Angptl8* accumulation in a time-dependent manner in cultured primary hepatocytes (Fig. 2a). In addition, both *Angptl8* mRNA levels and *Angptl8* protein levels were increased by overexpressing LXR α in primary hepatocytes (Fig. 2b,c). By contrast, CRISPR/Cas9-mediated knockout of *Lxr α* significantly attenuated *Angptl8* protein amounts in mouse liver (Fig. 2d). Additionally, we applied GSK2033 to block the activation of LXR α to pursue the role of LXR α in regulating *Angptl8* expression during refeeding status. As expected, refeeding-induced upregulation of *Angptl8* mRNA accumulation was significantly attenuated in the liver and WAT by GSK2033 administration (Fig. 2e). Correspondingly, both hepatic and plasma *Angptl8* protein levels were dramatically decreased (Fig. 2f). Together, these results demonstrate that LXR α plays a critical role in regulating *Angptl8* expression during feeding periods.

Identification of LXREs within the promoter region of *Angptl8* gene. To investigate the underlying mechanism of LXR α regulation of *Angptl8* expression, we constructed an *Angptl8* promoter-driven luciferase reporter plasmid. As luciferase reporter assay results suggested, overexpression of LXR α together with retinoid X receptor (RXR) enhanced the activity of *Angptl8* promoter-driven luciferase reporter (Fig. 3a). Since promoter analysis failed to identify any canonical LXR response elements (LXREs) in this promoter region of *Angptl8*, we then performed promoter-truncation analysis to reveal that the region from -1.8 to -2 kbp of *Angptl8* promoter was mainly responsible for LXR α -induced *Angptl8*-Luc expression (Fig. 3b). To further identify the binding site(s) of LXR α , we then made a series of deletions around four putative LXREs (denoted as pLXRE-1 to pLXRE-4, Fig. 3c). The results from luciferase reporter assay indicated that pLXRE-3 and pLXRE-4 were required for LXR α induction of *Angptl8*-Luc activity (Fig. 3d). Supporting these results, ChIP assay demonstrated that LXR α was present on these sites at ZT16 when *Angptl8* mRNA level was near its plateau (Fig. 3e).

Glucocorticoids negatively regulate *Angptl8* expression during fasting. To explore the mechanism of fasting-induced *Angptl8* repression, we analyzed the promoter region of *Angptl8* and noticed a palindromic sequence (cctcNNggag) of negative glucocorticoid response element (nGRE) that locates between -1096 bp and -1105 bp upstream of the transcriptional start site (TSS) of *Angptl8* gene. Coincidentally, plasma glucocorticoid profile was opposite with the expression pattern of *Angptl8* gene *in vivo* (Fig. 1a)²². We thus examined the role of glucocorticoids in regulating *Angptl8* expression. As shown in Fig. 4a, dexamethasone (DEX) treatment repressed the mRNA levels of *Angptl8* and *Nr1d1*, a known glucocorticoid-inhibited gene²³, in primary mouse hepatocytes. Correspondingly, *Angptl8* protein amounts decreased in a time-dependent manner after DEX treatment (Fig. 4b). In line with these *in vitro* results, *Angptl8* expression was suppressed in the liver and white adipose tissues (WAT) from mice intraperitoneally injected with DEX at ZT12, when plasma levels of glucocorticoids

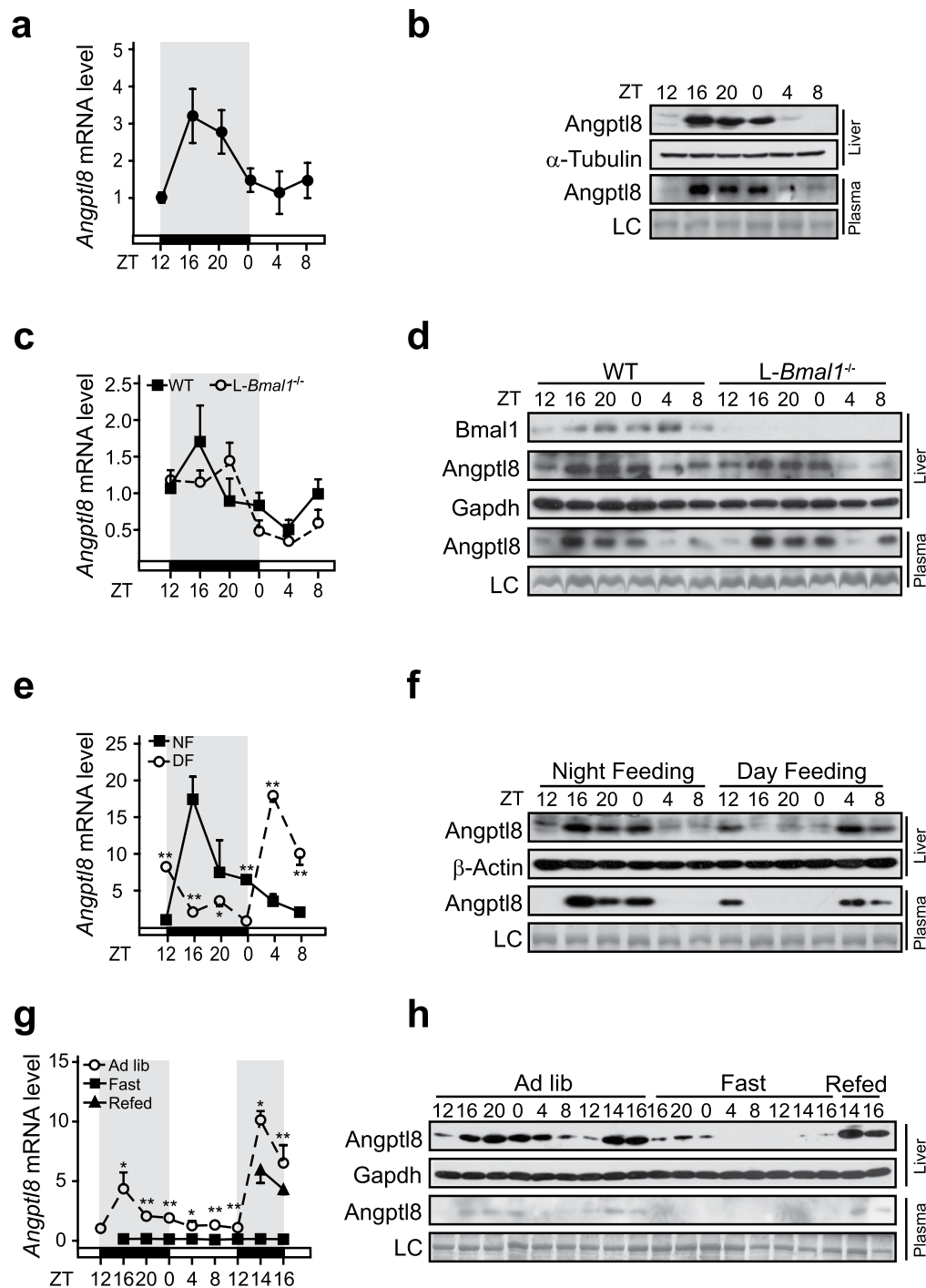


Figure 1. Food availability is a synchronizer of hepatic *Angptl8* oscillation. Ad libitum-fed liver-specific *Bmal1*-null mice and wild type littermates were euthanized at 4-hour intervals around the clock from Day1-ZT12 to Day2-ZT8. Liver and plasma samples were harvested. *Angptl8* mRNA and protein levels were measured by qPCR and immunoblot assay, respectively. Temporal profiles of hepatic *Angptl8* mRNA expression (a), as well as hepatic and plasma *Angptl8* protein accumulation, LC: loading control (b) in wild-type mice. (c) Temporal expression of hepatic *Angptl8* in mice of indicated genotypes. (d) Hepatic and plasma *Angptl8* protein accumulation profiles throughout the day. (e,f) Twelve-week-old male C57BL/6 mice were randomly separated into two groups: mice were provided food restrictively at nighttime (ZT12-ZT0, NF); or at daytime (ZT0-ZT12, DF), and then animals were euthanized at 4-hour intervals from Day2-ZT12 to Day3-ZT8. Liver and plasma samples were harvested. Temporal expression of *Angptl8* was analyzed by qPCR (e) and immunoblot assay (f). (g,h) Mice were randomly separated into three groups: for the fast group, mice were fasted from Day1-ZT12 to Day2-ZT20; for the refed group, mice were fasted for 24 h from Day1-ZT12 to Day2-ZT12 and then refed at Day2-ZT12; Mice fed ad libitum were served as controls. Animals were euthanized at 4-hour intervals around the clock from Day1-ZT12 to Day2-ZT20 as indicated. Temporal expression of *Angptl8* was analyzed by qPCR (g) or immunoblot assay (h). Data are represented as mean \pm s.e.m, $n = 3$, * $p < 0.05$, ** $p < 0.01$.

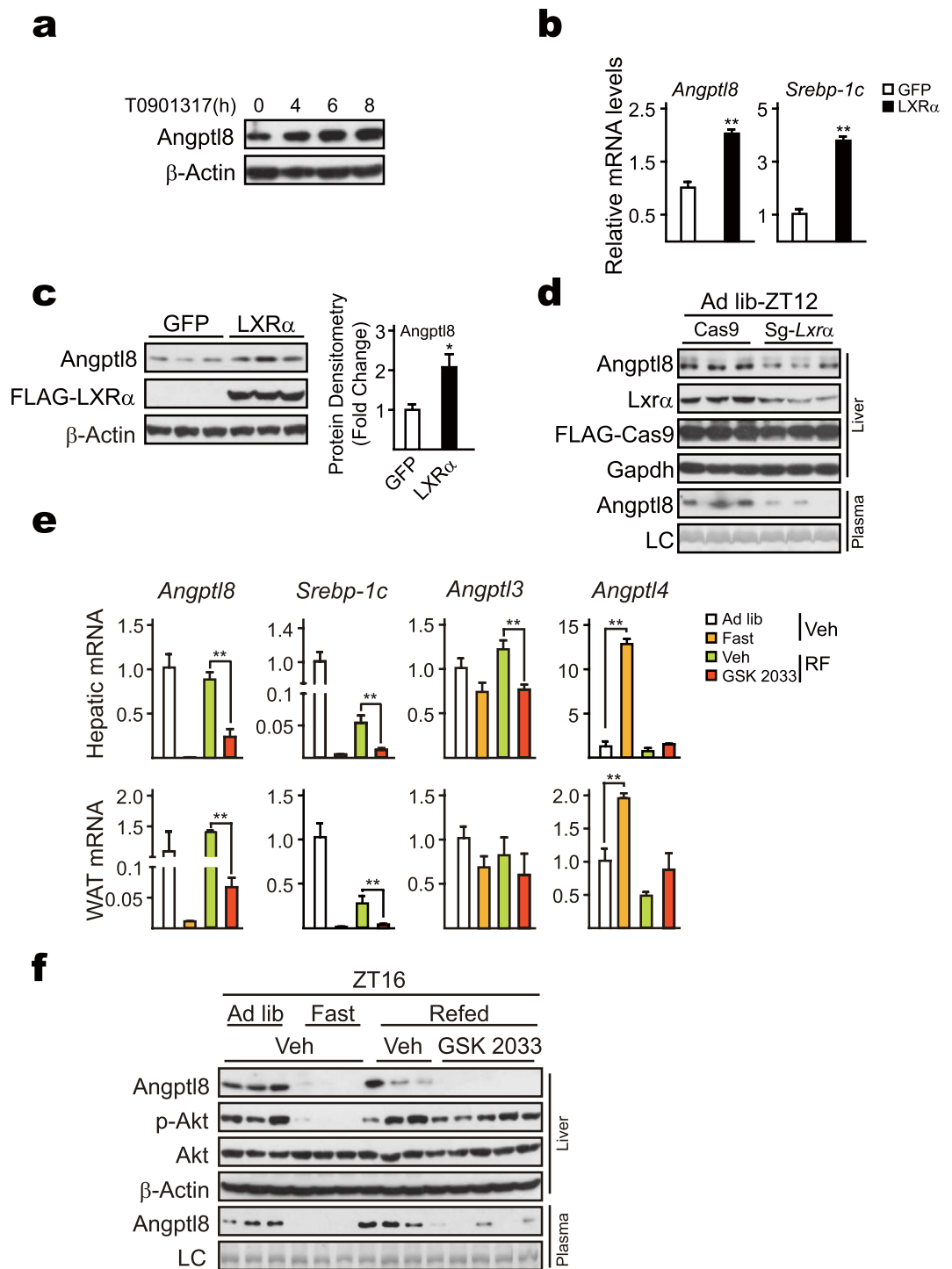


Figure 2. LXR α modulates *Angptl8* gene induction during refeeding. (a) T0901317 increases *Angptl8* accumulations in a time-dependent manner. Mouse primary hepatocytes were treated with T0901317 (10 nM) for the indicated time points, after which immunoblot assay was performed. (b,c) Cultured primary hepatocytes were infected with Ad-GFP or Ad-LXR α . The infected cells were cultured O/N in serum-free M199 medium and then treated with T0901317 (10 nM) for 4 hours. *Angptl8* expression was analyzed by qPCR (b), and immunoblot assay (c), respectively. (d) Knockout of *Lxr α* decreases *Angptl8* amounts *in vivo*. (e,f) Mice were randomly separated into four groups as indicated. For group 1, mice were fed ad libitum; for group 2, mice were fasted from Day1-ZT12 to Day2-ZT16; for two refed groups, mice were fasted from Day1-ZT12 to Day2-ZT12, followed by refed 4 h from Day2-ZT12 to Day2-ZT16. For the refed group, animals were intraperitoneally injected with vehicle (Veh) and GSK 2033 (20 mg/Kg) at Day2-ZT12, respectively. All animals were euthanized at Day2-ZT16. Liver and plasma samples were harvested. Temporal expression of *Angptl8* was analyzed by qPCR (e), and immunoblot assay (f), respectively. Data are represented as mean \pm s.e.m, n = 3–5, * p < 0.05, ** p < 0.01.

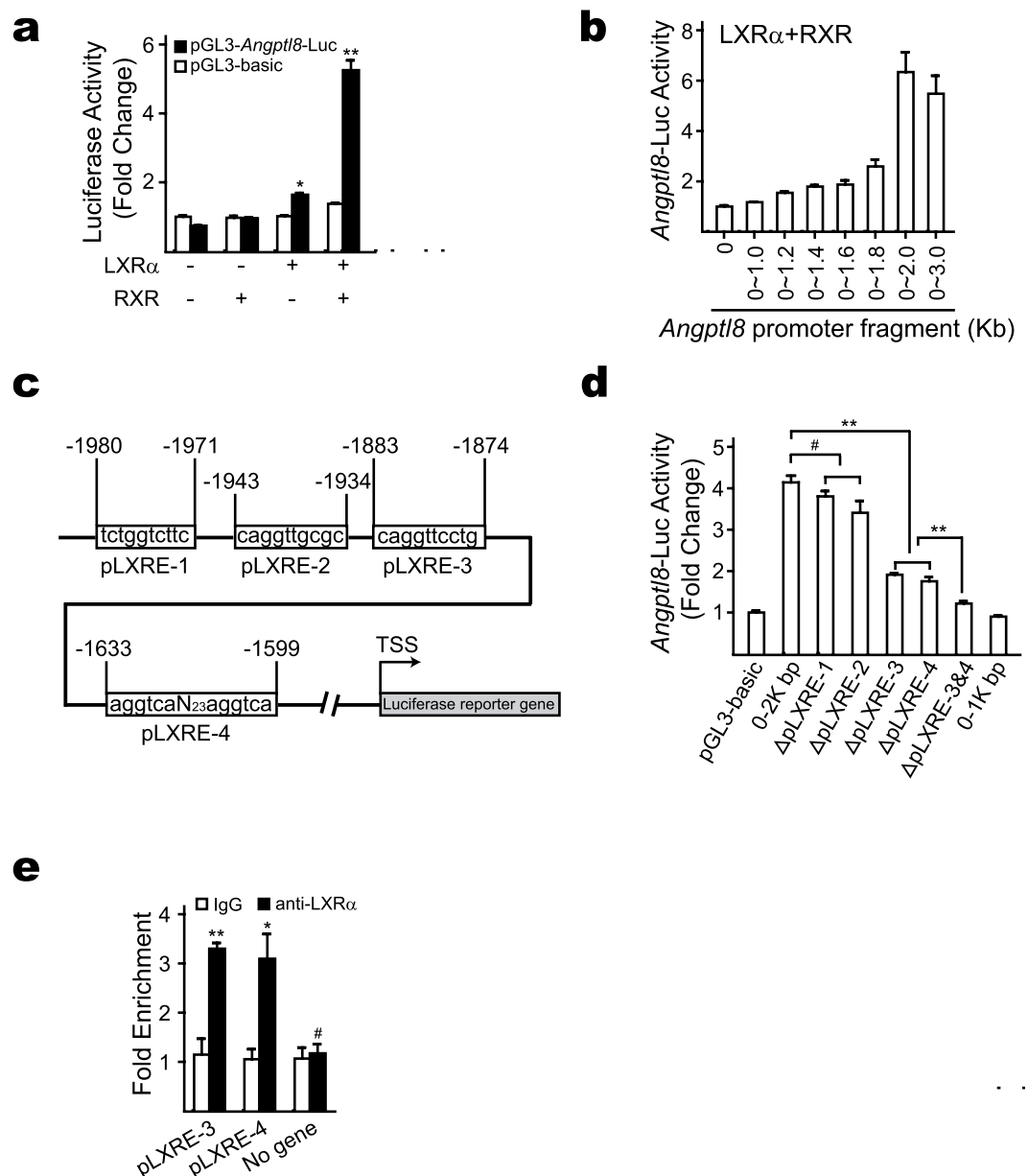


Figure 3. Identification of two non-canonical LXR response elements. (a) LXR α and RXR increase *Angptl8*-Luc activity. Indicated plasmids were co-transfected into HEK293T cells as specified and luciferase activity was measured and calculated as described in Methods. (b) *Angptl8* promoter truncation analysis. Reporter plasmids driven by different *Angptl8*-promoter fragments, LXR α , RXR and β -gal were co-transfected into HEK293T cells as indicated, then cells were lysed and assayed for firefly luciferase and β -gal activities. (c) Graphic of putative LXREs (pLXREs) in the promoter region of *Angptl8*. (d) *Angptl8* promoter deletion analysis. Reporter plasmids driven by different *Angptl8*-promoter regions (Δ : deletion), as well as LXR α , RXR and β -gal were co-transfected into HEK293T cells as indicated, then cells were lysed and assayed for firefly luciferase and β -gal activities. (e) ChIP analysis of the occupancy of LXR α on *Angptl8* pLXRE sites in livers of mice euthanized at ZT16. No gene serves as negative control. Data are represented as mean \pm s.e.m, n = 3, * p < 0.05, ** p < 0.01, # no significant difference.

begin to decrease²², and euthanized around ZT16, compared to those injected with control vehicle (Fig. 4c,d). To further verify the role of glucocorticoids in suppressing *Angptl8* expression, we applied mifepristone (RU486), a synthetic anti-glucocorticoid drug, to block the glucocorticoid signals *in vivo*. As expected, RU486 administration significantly attenuates fasting-induced *Angptl8* suppression both in the liver and WAT (Fig. 4e-g), without influencing plasma glucocorticoid levels (Fig. 4h). Together, these results suggest that glucocorticoid signals mediate fasting-induced *Angptl8* suppression.

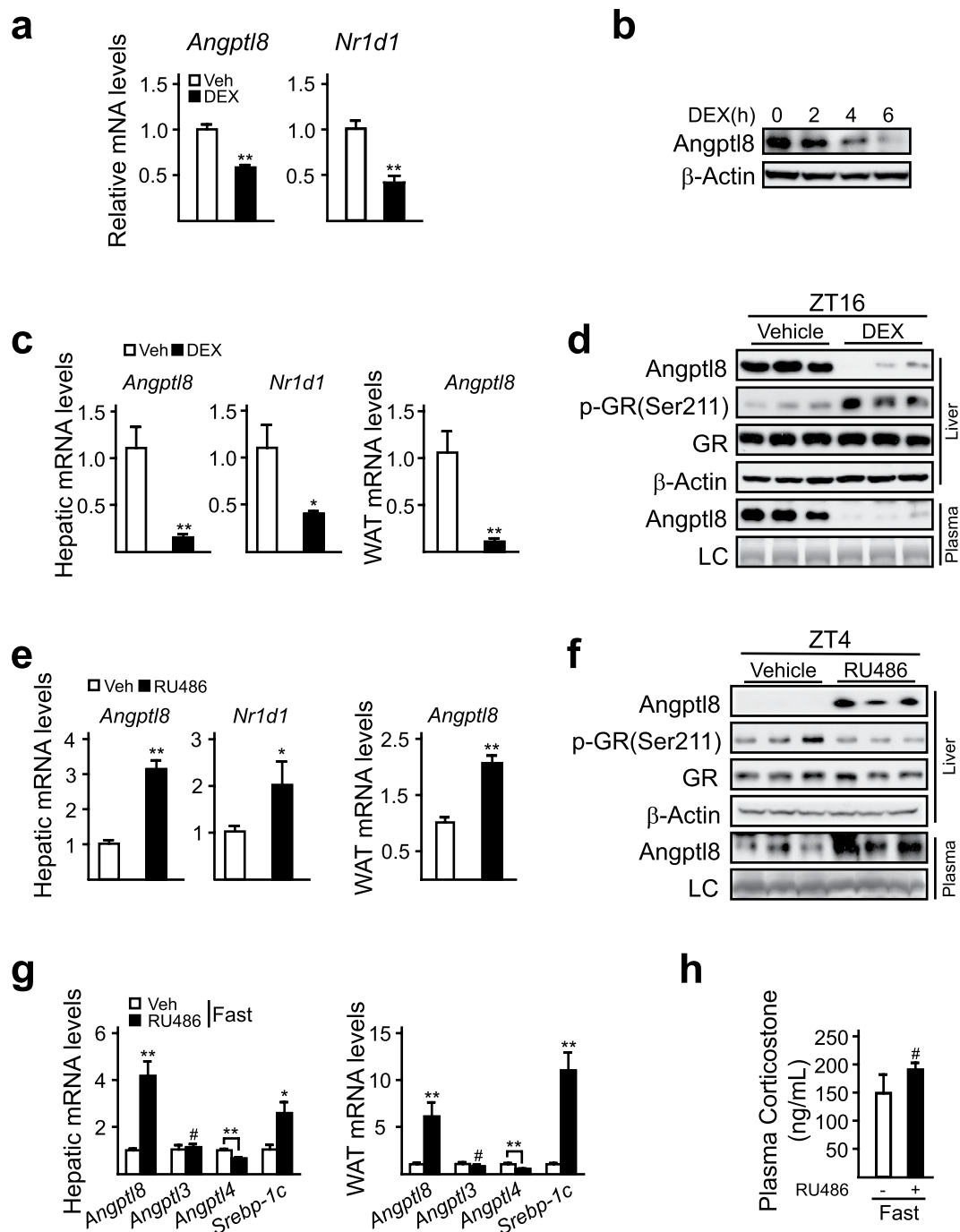


Figure 4. Glucocorticoids suppress *Angptl8* expression during fasting. (a) Quantitative PCR analysis of *Angptl8* mRNA levels in dexamethasone (DEX, 10 nM, 4 h) treated primary hepatocytes. (b) Immunoblotting analysis of *Angptl8* protein levels in primary hepatocytes treated with DEX (10 nM) for the indicated time points. (c,d) Ad libitum-fed C57BL/6 mice were intraperitoneally injected with vehicle (PBS) or dexamethasone (DEX, 2 mg/Kg) at ZT12, and then animals were euthanized at ZT16. Temporal expression of *Angptl8* was analyzed by qPCR (c), or immunoblot assay (d). (e,f) Ad libitum-fed mice were intraperitoneally injected with vehicle (PBS) or RU486 (20 mg/Kg, n = 5) at ZT0, and then animals were euthanized at ZT4. Temporal expression of *Angptl8* was analyzed by qPCR (e), or immunoblot assay (f). (g,h) Mice were intraperitoneally injected with vehicle (PBS) or RU486 (20 mg/Kg) at ZT12, then animals were kept fasting and euthanized at ZT16. qPCR analysis of *Angptl3*, 4, 8 and *Srebp-1c* mRNA levels (g). Plasma glucocorticoid levels (h). Data are represented as mean \pm s.e.m, * $p < 0.05$, ** $p < 0.01$, # no significant difference.

GR mediates the inhibitory effect of glucocorticoids on *Angptl8* expression. Since the biological effects of glucocorticoids are mainly conferred by their cognate intracellular receptor, glucocorticoid receptor (GR), we then examined the necessity of GR in the suppression of *Angptl8* expression induced by glucocorticoids.

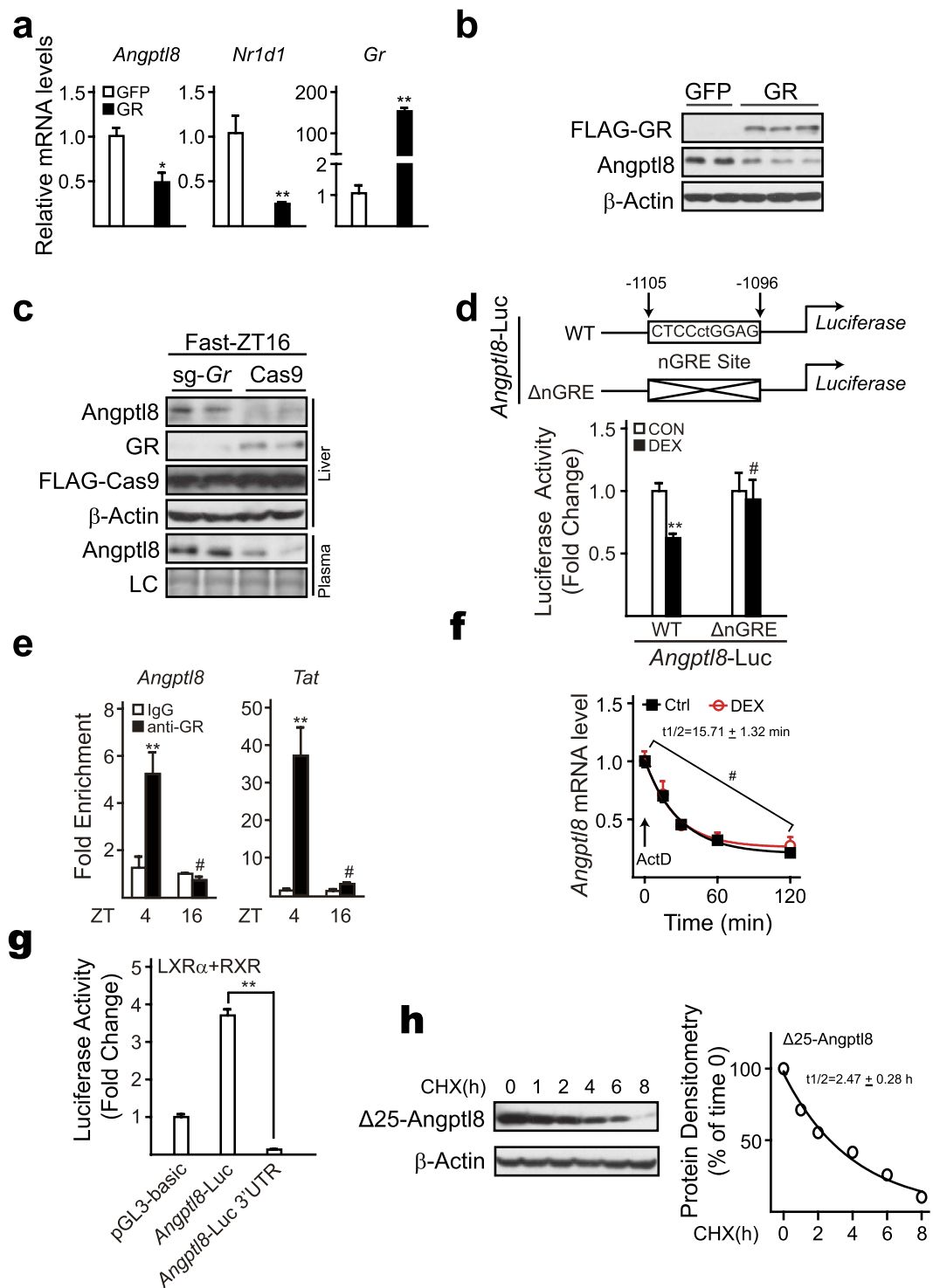


Figure 5. Identification of nGRE element in *Angptl8* promoter region. Cultured mouse primary hepatocytes were infected with Ad-GFP and Ad-GR virus, respectively. The infected cells were cultured overnight (O/N) in serum-free M199 and then treated with DEX (10 nM) for 4 hours. *Angptl8* mRNA levels (a), and Angptl8 protein amounts (b) were analyzed by qPCR and immunoblot, respectively. (c) Knockout of *Gr* ameliorates Angptl8 reduction caused by fasting. Cas9 alone or sg-*Gr*-Cas9 adenoviruses were delivered into livers of adult C57BL/6 mice by tail-vein injection on Day1, and then animals were fasted at Day15-ZT12, euthanized at Day15-ZT16. Liver and plasma samples were harvested and immunoblot assay was performed to detect Angptl8 protein levels. (d) The nGRE site is necessary for *Angptl8* to response to DEX treatment. Reporter plasmid (*Angptl8*-WT-Luc or *Angptl8*-ΔnGRE-Luc, up) and RSV-β-gal plasmid were co-transfected into HEK293T cells. The transfected cells were cultured O/N in serum-free DMEM and then treated with vehicle (PBS) or DEX (10 nM) for 4 hours. Luciferase activities were measured and normalized to β-gal activity (bottom). (e) ChIP analysis of the occupancy of GR on *Angptl8* nGRE site in livers of ad libitum-fed mice euthanized at ZT4 and

ZT16. *Tat* here serves as a positive control. (f) Half-life of *Angptl8* mRNA. Cultured primary hepatocytes were treated with actinomycin D (ActD, 5 μ g/ μ L) or ActD plus DEX (10 nM) for the indicated time points. *Angptl8* mRNA levels were then analyzed by qPCR and *Angptl8* mRNA half-life was calculated by using one phase decay equation. (g) 3'-UTR of *Angptl8* takes responsibility for *Angptl8* mRNA instability. HEK293T cells were transfected with *Angptl8*-Luc and *Angptl8*-Luc-3'UTR, respectively. The transfected cells were left overnight, and then lysed and assayed for firefly luciferase and β -gal activities. (h) HEK293T cells were transfected with Δ 25- *Angptl8* (*Angptl8* without signal peptide) plasmids, then cultured O/N in serum-free DMEM and treated with cycloheximide (CHX, 10 μ g/mL) for the indicated time points, after which immunoblot assay was performed (left) and Δ 25- *Angptl8* half-life was calculated by using one phase decay equation (right). Data are represented as mean \pm s.e.m, n = 3, * p < 0.05, ** p < 0.01, # no significant difference.

Indeed, adenoviral overexpression of GR markedly augmented the reduction of *Angptl8* expression induced by DEX-treatment in cultured primary hepatocytes (Fig. 5a,b). We further verified such effect *in vivo* by using adenovirus-delivered CRISPR/Cas9-GR system in mouse liver. As expected, Ad-CRISPR/Cas9-mediated liver-specific *Gr* deficiency significantly diminished fasting-induced suppression of hepatic *Angptl8* expression (Fig. 5c). To map the binding site(s) of GR on *Angptl8* promoter, we then constructed a plasmid expressing a luciferase reporter driven by either the wide-type promoter region of *Angptl8* gene (2000 bp upstream ahead of the TSS, *Angptl8*-WT-Luc) or a corresponding nGRE-deletion mutant one (*Angptl8*- Δ nGRE-Luc, Fig. 5d, up). As a result, DEX significantly reduced the activity of *Angptl8*-WT-Luc in HEK293T cells, but not that of *Angptl8*- Δ nGRE-Luc (Fig. 5d, bottom). Consistently, results of chromatin immunoprecipitation (ChIP) assay demonstrated that GR was dynamically recruited to the nGRE site within *Angptl8* promoter region in the liver (Fig. 5e), which accounts for the different transcriptional level of *Angptl8* between ZT4 and ZT16. Conclusively, these results confirm that GR binds directly to the nGRE element within *Angptl8* promoter region to mediate the inhibitory effect of glucocorticoids on *Angptl8* expression.

***Angptl8* mRNA decays rapidly after transcription.** Considering that mRNA/protein instability is the nature of almost all of the circadian genes, the rapidly turnover of *Angptl8* expression between fasting/feeding transitions promoted us to examine the half-life of its mRNA. Supporting this notion, *Angptl8* mRNA levels rapidly dropped after actinomycin D (ActD) treatment and its half-life was just approximately 15.71 min, which was independent of glucocorticoid signaling (Fig. 5f). As the 3'- untranslated region (3'-UTR) has been shown to play a major role in harboring determinants to control mRNA decay^{24,25}, we constructed a chimeric plasmid that replaces the luciferase reporter 3'-UTR with that of mouse *Angptl8* (pGL3-*Angptl8*-3'-UTR) to determine whether the *Angptl8* 3'-UTR is involved in the regulation of its mRNA stability. Strikingly, the luciferase activity of pGL3-*Angptl8*-3'-UTR was almost abolished, compared to that of control luciferase reporter (Fig. 5g). In addition, we examined *Angptl8* protein stability with a plasmid encoding *Angptl8* protein without signal peptide (Δ 25- *Angptl8*) to avoid the influence of secretion. As shown in Fig. 5h, *Angptl8* protein was relatively stable, with the half-life of approximately 2.47 h, compared to its mRNA stability. Together, these results suggest that the *Angptl8* mRNA instability contributes to the rapid response of *Angptl8* expression to fasting/feeding transitions, while the *Angptl8* protein stability makes it possess the capability to exert its function after secretion.

Effects of hepatic overexpression of *Angptl8* on glucocorticoid-regulated lipid metabolism.

Considering that chronically elevated glucocorticoid levels lead to non-alcoholic fatty liver^{26,27}, whereas the expression of *Angptl8* is inhibited by glucocorticoid signal, we wondered whether *Angptl8* plays a role in this regard. To answer this question, we overexpressed GFP, *Angptl8* or Δ 25- *Angptl8* in the liver by tail-vein delivery of corresponding adenoviruses on day 1, and then injected these mice with either DEX or PBS once-daily for three days from day 4 to day 6. Expression of *Angptl8* and Δ 25- *Angptl8* were readily detectable after 10-days post-injection (Fig. 6a). Surprisingly, overexpression of *Angptl8* didn't ameliorate fatty liver development in the mice with DEX injection (Fig. 6b), whereas, plasma TG and NEFA levels were dramatically elevated in these animals (Fig. 6c), resulting in cream-like plasma (Fig. 6d). These data imply a key role of *Angptl8* in plasma TG clearance and adipose TG mobilization in the context of DEX injection. Supporting this idea, we found that many genes involved in fatty acid synthesis, NEFA uptake, VLDL secretion were upregulated in the liver by overexpressing *Angptl8* (Fig. 6e), which accounts for the accelerated hepatic VLDL secretion rate (Fig. 6f). Intriguingly, ectopic expression of Δ 25-*Angptl8* exhibited similar effect as *Angptl8* overexpression (Fig. 6e), which implies an intracellular functional role of *Angptl8* in modulating gene transcription. Moreover, overexpression of *Angptl8* exerted no significant influence on transcription of gluconeogenesis-related genes, e.g. *G6p* and *Pepck* (data not shown), which is consistent with the knowledge that *Angptl8* does not impair glucose homeostasis^{13,19}. Of note, overexpression of *Angptl8* promotes lipolysis in adipocytes with DEX-treatment (Fig. 6g). Supporting these results, we noticed that *Atgl* and *Fatp4*, two genes involved in adipose TG mobilization and NEFA secretion, respectively, were upregulated in these regards (Fig. 6h). Taken together, these results confer a vital role of *Angptl8* in modulating TG homeostasis and suggest a tightly metabolic interaction between *Angptl8* and glucocorticoid signaling.

Discussion

Angptl8 accumulation is intimately linked with circulating TG contents, and emerging evidence implies a key role of *Angptl8* in the metabolic transition between fasting and feeding¹³. In the present study, we show that LXR α heterodimerizes with RXR to initiate the transcription of *Angptl8* induced by refeeding. On the other hand, glucocorticoids suppress *Angptl8* transcription by activating and subsequent recruiting GR dimmers to the nGRE

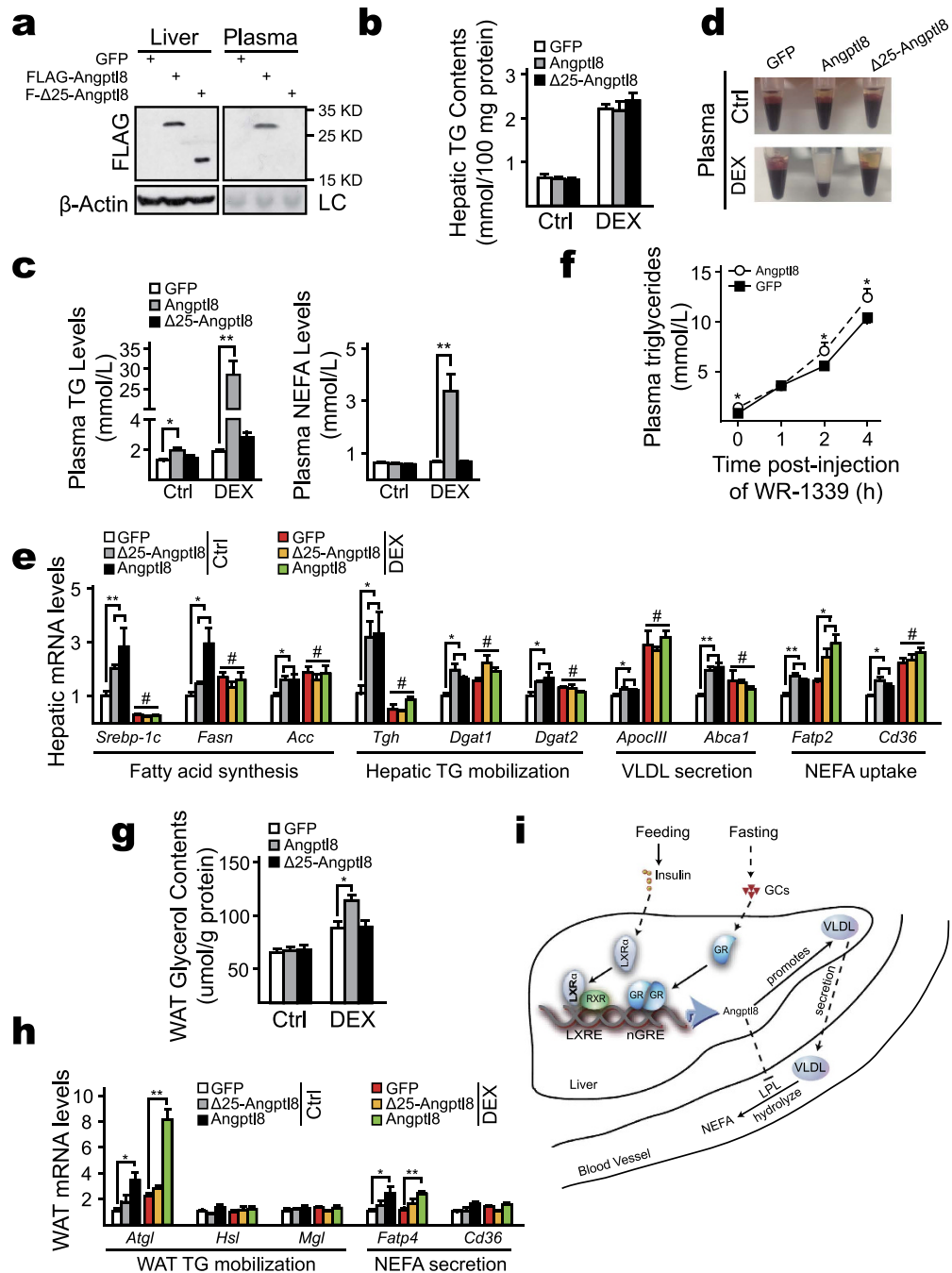


Figure 6. Metabolic interaction between Angptl8 and glucocorticoid signaling. Ad-GFP, Ad-Angptl8 or Ad-Δ25-Angptl8 adenoviruses were delivered into mice via tail-vein injection on Day1. Mice were treated with vehicle (PBS) or DEX (100 mg/Kg) by intraperitoneal injection once-daily for 3 days from Day4 to Day6, and then animals were euthanized on Day10. **(a)** Immunoblotting analysis of hepatic and plasma Angptl8 and Δ25-Angptl8. **(b)** Measurement of hepatic TG contents. **(c)** Measurement of plasma TG and NEFA levels of indicated virus-infected mice. **(d)** A picture of plasma shows that ectopic expression of Angptl8 results in cream-like plasma in DEX-treated mice. **(e)** Quantitative PCR analysis of mRNA levels of hepatic genes involved in lipid metabolism. **(f)** Plasma TG levels post-injection of Triton WR-1339 (500 mg/Kg) at the indicated time points. **(g)** Overexpressing Angptl8 promotes lipolysis in adipocytes in DEX-treated mice $n = 4-8$, * $p < 0.05$, ** $p < 0.01$, # no significant difference. **(h)** Overexpressing Angptl8 affects gene expression involved in lipolysis in WAT. **(i)** Hypothetical model showing the mechanism of fasting and feeding signals modulate Angptl8 expression in mouse liver. Postprandially, the liver X receptor alpha (LXR α) heterodimerizes with retinoid X receptor (RXR) and binds to the liver X receptor response element (LXRE) in the promoter of Angptl8 to initiate its transcription. During fasting state, elevated glucocorticoids suppress Angptl8 transcription by activating glucocorticoid receptor (GR) and subsequent binding of GR dimmers to the negative glucocorticoid response element (nGRE) in the promoter of Angptl8. Elevated Angptl8 increases plasma TG concentration, whereby promoting hepatic VLDL secretion and decreasing VLDL hydrolyzation via inhibiting LPL activity.

element within *Angptl8* promoter region during fasting. In addition, our data confer the specific role of Angptl8 in mediating plasma TG clearance, as well as modulating VLDL secretion (Fig. 6i).

The instability of *Angptl8* mRNA (~15.71 min, Fig. 5f) is vital for *Angptl8* oscillations and functions. Specifically, it allows the rapid response of *Angptl8* expression to fasting-feeding transition, which is involved in the generation of the circadian rhythm of its mRNA, as well as intracellular and plasma protein oscillations. Moreover, this nature of *Angptl8* mRNA fits its role in regulating lipid metabolism that is quickly and dramatically altered by eating. On the other hand, the relative high stability (~2.47 h, Fig. 5h) permits Angptl8 protein to be secreted and exert its function.

Although the circadian oscillation of *Angptl8* expression is not controlled directly by the peripheral core clock machinery, it is generated by feeding behaviors that are governed by the central clock locating in the suprachiasmatic nucleus²⁸. Furthermore, the production and secretion of glucocorticoids, which is the key inhibitory regulator of *Angptl8* expression, are under the control of the circadian clock²⁹. Thus, the rhythmic expression of *Angptl8* is affected indirectly by the molecular clock. In addition, we notice that hepatic Angptl8 protein abundances are slightly reduced in liver-specific *Bmal1*-knockout mice, compared to those in WT littermates (Fig. 1d), which may be due to the reduced protein synthesis caused by *Bmal1* deficiency³⁰.

LXRs (α/β) have been shown to play critical roles in the transcriptional regulation of lipid metabolism. For instance, activation of LXRs increases hepatic fatty acid synthesis, VLDL secretion to result in hypertriglyceridemia³¹. Intriguingly, both *Angptl8* and *Angptl3* are primary targets of LXRs³², and *Angptl3* function together with Angptl8 to inhibit plasma TG clearance¹¹. On the other hand, *Angptl3* expression is modestly altered by feeding behaviors³³, whereas *Angptl8* is dramatically affected by nutritional status¹⁵. It seems that Angptl8 functions as a responder to fasting and feeding signals and cooperates with Angptl3 to maintain lipid homeostasis. Taken together, these evidences reveal an intuitively mechanism of Angptl3/ Angptl8-mediated hypertriglyceridemia induced by LXRs.

An intriguing cognition seems clear about how glucocorticoids and LXRs regulate plasma TG trafficking whereby modulating the expression of *Angptl3*, 4, and 8. Although no significant change happens on *Angptl3* transcription during fasting (Fig. 2e), *Angptl8* is dramatically suppressed Fig. 1g–h and Fig. 2e, whereas *Angptl4* is upregulated due to the elevated circulating glucocorticoid levels³⁴. On one hand, reduced amounts of the Angptl8 protein augments LPL activity specifically in heart and skeletal muscles³⁵, and thus promotes the hydrolysis of VLDL-TG to result in the increased circulating NEFA concentrations. On the other hand, increased amounts of Angptl4 protein decreases LPL activity in an adipose-specific manner³⁶, and promotes intracellular lipolysis in adipocytes³⁷. Together, decreased adipose-LPL activity and enhanced muscle-LPL activity direct the flux of circulating TG toward peripheral tissues for utilization. Such fasting scenario is completed reversed under feeding status. Briefly, feeding-induced activation of LXRs and decrease of circulating glucocorticoids lead to the upregulation of *Angptl8* and downregulation of *Angptl4*. As a result, plasma TG is directed to adipose tissues for storage. Supporting this notion, Angptl3 has been suggested to be involved in the redirection of TG to adipose tissue for storage during feeding, whereas the postprandial increase in TG delivery to adipose tissue is abolished in mice lacking *Angptl8*⁷.

Consistent with previous report that the absence of *Angptl8* profoundly disrupts VLDL secretion¹³, our data demonstrate that overexpression of Angptl8 in mouse livers upregulates hepatic genes involved in lipid metabolism (Fig. 6e), which considerably accelerates VLDL secretion (Fig. 6f). However, such effect of Angptl8 overexpression is almost abolished by DEX injection (Fig. 6e), which may be due to the dominant impact of DEX on these gene expressions diminishes the difference between Ad-GFP- and Ad- Angptl8-infected mice. Although the secretion rate was accelerated, hepatic TG contents were identical between GFP and Angptl8 overexpressed mice. One of the possible explanations is that the whole process of lipid metabolism from NEFA uptake to hepatic TG synthesis, VLDL-TG incorporation and secretion is accelerated by Angptl8 overexpression, which results in the balance of TG homeostasis in the liver, but the great TG accumulation in the plasma. In addition, we notice that *Angptl8* deficiency doesn't impair the expression of lipid biosynthesis genes, such as *Srebp-1c* and *Acc1*¹³, which is inconsistent with the results of overexpressing Angptl8 described in this study. One possible explanation for this discrepancy is that there may be other factors that can compensate the intracellular function of Angptl8.

Of note, ectopic expression of wild-type Angptl8, rather than a mutant one lacking the signal peptide responsible for secretion ($\Delta 25$ -Angptl8), results in markedly increased plasma TG and NEFA levels in DEX-treated mice (Fig. 6c,d). One of the most likely explanations for this strong phenotype is that the highly expressed Angptl8 and Angptl4 in such circumstance diminish plasma TG clearance to cause sustained circulating TG accumulation, as suggested by the Angptl3-4-8 model³⁸. Besides, overexpression of Angptl8 upregulates *Atgl* and *Fatp4* gene expression (Fig. 6h) to prompt lipolysis in adipocytes in DEX-injected mice (Fig. 6g) to result in the dramatically elevated plasma NEFA levels (Fig. 6c). These data further suggest a close metabolic interaction between Angptl8 and glucocorticoid signaling in adipose tissue. Moreover, ectopically overexpressing $\Delta 25$ -Angptl8 exhibits similar effect on lipid metabolism-related gene expression as Angptl8 (Fig. 6e), implying an intracellular functional role of Angptl8 in modulating gene transcription. Further investigations are needed to explore the functional role of Angptl8 in these regards.

Materials and Methods

Mice and treatments. Eight- to twelve-week-old C57BL/6J male mice were purchased from Shanghai Laboratory Animal Centre (China) and housed in the animal facility at Shanghai Institutes for Biological Sciences (SIBS). Mice were maintained on a 12-h light/12-h dark cycle for at least 2 weeks before study and had free access to water and regular diet (12% fat/68% carbohydrate/20% protein). For time-restricted feeding experiment: mice under daytime-restricted feeding (DF) were provided food during the entire light period (7:00 AM–7:00 PM), whereas nighttime-restricted feeding (NF) mice were provided food only at dark time (7:00 PM–7:00 AM). Experimental schedule of fasting and refeeding experiments has been described²². For hepatic Angptl8

overexpression study, recombinant adenoviruses were delivered into mice by tail vein injection, and then animals were intraperitoneally injected with PBS or DEX (100 mg/Kg) for successive three days from day 4 to day 6 and euthanized on day 10 post-injection. For other *in vivo* experiments, mice were treated as described specifically in Figure Legends. All research procedures were performed in accordance with the guidelines and regulations, as well as ethically approved by the Animal Care and Use Committee of the Institute for Nutritional Sciences.

Cell culture. HEK293T cells were purchased from American Type Culture Collection (ATCC). Mouse primary hepatocytes were isolated by using collagenase (Sigma) and plated on dishes pre-coated with rat tail tendon collagen (Sigma) according to manufacturers' instructions. HEK293T cells and primary hepatocytes were cultured in Dulbecco's Modified Eagle's Medium (DMEM) and medium 199 (M199), respectively. Complete medium containing 10% fetal bovine serum and 1% penicillin/streptomycin. HEK293T cells were transfected by using PEI (Sigma) reagent according to manufacturers' instructions. Briefly, plasmid (ug) and PEI reagent (1 ug/ μ L) were mixed in a ratio of 1:3, and then incubated for 15 min at room temperature. Medium was changed into serum-free DMEM, and then PEI/Plasmid transfection complexes were added into wells. Cells were lysed for western blot or luciferase activity analysis after 24 hours post-transfection. Primary hepatocytes were synchronized by serum starvation for overnight and then infected by adenovirus as specified.

Plasmid. The expression plasmids used in this study were generated according to standard molecular biology techniques. For luciferase reporter plasmid construction, the mouse *Angptl8* genomic fragments were amplified by polymerase chain reaction (PCR) with specific primers. The amplified PCR products were separated using DNA agarose gel and recovered using QIAquick Gel Extraction Kit (cat. 28706), then digested with corresponding restriction enzymes. The prepared PCR products were then linked into pGL3-basic reporter plasmid, which was previously digested with the same restriction enzymes as used to digest PCR products. *Angptl8*, *Lxr α* , *et al.* were amplified and cloned into pcDNA plasmid by using the same method as mentioned above. All the plasmids were subjected to sequencing for verification. Primers used for cloning were provided in Supplementary Table 1.

Immunoblot Assay. For immunoblot analysis, cultured cells or harvested liver tissues were lysed in RIPA buffer containing proteinase inhibitors (PMSF, Cocktail and Phosphatase Inhibitors), followed by centrifuging at 12,000 r.p.m for 15 min at 4 °C. Supernatants were collected and protein concentrations were determined by using BCA protein assay kit (Pierce, 23225) according to manufacturers' instruction. Took same amounts of total protein from the left supernatants, then added corresponding volume of lysis buffer and 5x SDS loading buffer to make the final protein concentration identical, then boiled for 10 min. Identical amounts of protein were subjected to SDS-PAGE electrophoresis and transferred to methanol-activated polyvinylidene fluoride membranes (PVDF, Millipore). Membranes were then blocked with 5% milk for 1 h at room temperature and incubated overnight with corresponding primary antibodies at 4 °C, then with secondary antibodies for 1 h at room temperature. Finally, the protein bands were developed by using ECL western blotting substrate (Thermo Pierce) and visualized with western film processor. Primary antibodies used in this study were as follows: Bmal1 (ab3350, Abcam, 1:1000), pSer473-Akt (#9271, CST, 1:1000), Akt (#9272, CST, 1:1000), GR (ab3578, Abcam, 1:1000), LXR α (ab41902, Abcam, 1; 1000), FLAG-HRP (A8592, Sigma, 1:5000), *Angptl8* (generated by using the epitope of EFETLKARADKQ, 1:500), and β -Actin (#4967, CST, 1:6000).

Adenoviruses. We applied CRISPR/Cas9 system to explore the effects of GR and LXR α on *Angptl8* expression. Single-guide RNAs used to mediate site-specific gene mutation by Cas9 were designed according to previously described³⁹. We synthesized the designed sgRNAs and inserted them into the reconstructed pShuttle plasmids that contain U6 promoters for sgRNA expression and Cas9 coding sequence. Adenoviruses encoding *Angptl8*, GR, LXR α , green fluorescent protein (GFP), gene specific single-guide RNA (sg-GR, sg-LXR α) and Cas9 alone (sg-Cas9) were generated using AdEasy system as previously described⁴⁰. Sequences of sg-RNAs used to mediate gene specific knock-out were as follows:

sgRNA-GR-Guide: CACCGACGGCTGGTCGACCTATTG,
 sgRNA-GR-Comp: AAACCAATAGGTCGACCAGCCGTC;
 sgRNA-LXR α -Guide: CACCGTGGGCAAGGCGTGACGCGC
 sgRNA-LXR α -Comp: AAACGCGCGTCACGCCTTGGCCAC.

Total RNA isolation and qPCR analysis. Total RNAs from liver or cultured primary hepatocytes were extracted using Trizol reagents (Invitrogen). The mRNAs were then reverse-transcribed into cDNA by the primer scriptTM RT reagent kit with gDNA eraser (Takara) according to manufacturers' protocol. Relative mRNA levels were determined by SYBR Green RT-PCR kit (Takara) with ABIPRISM 7900HT sequence detector (Perkin Elmer). Real-time PCR data were analyzed by the comparative C_T method⁴¹. Ribosomal L32 mRNA levels were used as internal control. Primers used for qPCR analysis were provided in Supplementary Table 2.

Chromatin Immunoprecipitation (ChIP). Liver tissues were cross-linked with 1% formaldehyde. GR or LXR α antibodies were used for immunoprecipitation (IP) along with rabbit IgG for negative controls. After removing cross-link, DNA was extracted using phenol-chloroform and ethanol precipitated. Target promoters were analyzed using SYBR Green Real-time PCR and normalized to input chromatin signals. Primer sequences used in these experiments were provided as follows (5'-3'):

GR -ChIP-F: TAAGGTGGTCCCACCAGTAG;
 GR -ChIP-R: CAGGTTCCGGTTCTCTTTGT.
 LXR α -ChIP-F3: GTGTGGGTACACGAAGAGCA;
 LXR α -ChIP-R3: GAGGTTCCACCCACTGTCTG.

LXR α -ChIP-F4: TCCTGGTCTACATAGCAAGT;
 LXR α -ChIP-R4: CTAAATAGCAAACCTCAGATC.
 ChIP primers used for *Tat* and *No Gene* were as previously described^{42,43}.

Luciferase activity assay. Cells were collected after 24 hours post-transfection and lysed using lysis buffer (Gly-gly buffer: 25 mM Gly-gly, pH 7.8; 15 mM MgSO₄; 4 mM EGTA, pH 7.8; 1 mM DTT and 1% V/V Triton X-100). For 24-well plate, we added 150 μ L of lysis buffer to each well, and then shook gently for 20 minutes by transference decoloring shaker. Mixed 50 μ L of lysate with 50 μ L of assay mix (20 mM Gly-gly, pH 7.8; 12 mM MgSO₄; 3 mM EGTA, pH 7.8; 0.2 mM Potassium Phosphate, pH 7.8; 2 mM ATP; 1.5 mM DTT and 1.25 mg/mL firefly luciferin) in a well of a black 96-well plate. Fluorescence intensity was measured using the equipment of Luniscan Ascent (Thermo). For β -gal assay to normalize the luciferase assay results, another 50 μ L per well of lysate was taken to be mixed with 50 μ L per well of β -gal solution, incubated at room temperature until color developed, and then read A420 on a plate reader (Epoch Microplate Spectrophotometer, BioTek).

TG and NEFA measurement. To measure hepatic TG, we balanced approximately 100 mg of liver tissue and added 500 μ L of cold PBS, then homogenized in a 1.5 mL eppendorf tube on ice. 200 μ L of homogenates were transferred into a new tube and mixed with 800 μ L of chloroform/methanol (2:1, v/v) adequately, then followed by centrifuging at 2500 r.p.m for 10 min at 4 °C. Quitted upper water-phase and transferred lower organic phase into a new tube, evaporated to dryness overnight in a chemical hood. The evaporated samples were then resuspended in 800 μ L of EtOH-Triton X-100 (1% Triton X-100 in absolute ethanol), then TG contents were measured using commercial assay kit (SHENSUO UNF, China). Remainder of each homogenate was used to determine protein concentrations by using BCA protein assay kit (Pierce, 23225) according to manufacturers' instruction. The final TG contents were normalized with corresponding protein concentrations. For plasma TG and NEFA measurement, bloods were harvested after mice were euthanized and plasma samples were prepared. Plasma TG and NEFA were determined with TG kit (SHENSUO UNF, China) and Wako HR Series NEFA-HR kit (Wako Pure Chemical Industries, Ltd), respectively.

Statistical Analyses. Results were represented as mean \pm s.e.m. The comparisons of two groups of mice or different primary hepatocytes preparations were carried out using two-tailed unpaired Student's *t* test. Differences were considered statistically significant at $P < 0.05$. No statistical methods were used to predetermine sample size. All experiments were performed on at least two independent occasions.

References

- Osono, Y., Nakajima, K. & Hata, Y. Hypertriglyceridemia and fatty liver: clinical diagnosis of fatty liver and lipoprotein profiles in hypertriglyceridemic patients with fatty liver. *J. Atheroscler Thromb.* **2**, 47–52 (1995).
- Grundy, S. M. Hypertriglyceridemia insulin resistance and the metabolic syndrome. *Am J Cardiol.* **83**, 25–29 (1999).
- Marleen, M. J. *et al.* Chylomicron synthesis by intestinal cells *in vitro* and *in vivo*. *Atherosclerosis.* **141**, 9–16 (1998).
- Gibbons, G. F. *et al.* Synthesis and function of hepatic very-low-density lipoprotein. *Biochem Soc Trans.* **32**, 59–64 (2004).
- Franssen, R. *et al.* Role of lipoprotein lipase in triglyceride metabolism: potential therapeutic target. *Future lipidol.* **3**, 385–397 (2008).
- Oike, Y., Akao, M., Kubota, Y. & Suda, T. Angiotensin-like proteins: potential new targets for metabolic syndrome therapy. *Trends Mol Med.* **11**, 473–479 (2005).
- Mattijssen, F. & Kersten, S. Regulation of triglyceride metabolism by Angiotensin-like proteins. *Biochim Biophys Acta.* **1821**, 782–789 (2012).
- Inaba, T. *et al.* Angiotensin-like protein 3 mediates hypertriglyceridemia induced by Liver X receptor. *J. Biol Chem.* **278**, 21344–21351 (2003).
- Koster, A. *et al.* Transgenic angiotensin-like (angptl)4 overexpression and targeted disruption of angptl4 and angptl3: regulation of triglyceride metabolism. *Endocrinology.* **146**, 4943–4950 (2005).
- Lafferty, M. J. *et al.* Angiotensin-like protein 4 inhibition of lipoprotein lipase: evidence for reversible complex formation. *J Biol Chem.* **288**, 28524–28534 (2013).
- Quagliarini, F. *et al.* Atypical angiotensin-like protein that regulates ANGPTL3. *Proc Natl Acad Sci USA.* **109**, 19751–19756 (2012).
- Fu, Z. *et al.* Lipasin, thermoregulated in brown fat, is a novel but atypical member of the angiotensin-like protein family. *Biochem Biophys Res Commun.* **430**, 1126–1131 (2013).
- Wang, Y. *et al.* Mice lacking ANGPTL8 (Betatrophin) manifest disrupted triglyceride metabolism without impaired glucose homeostasis. *Proc Natl Acad Sci USA.* **110**, 16109–16114 (2013).
- Kersten, S. *et al.* Characterization of the fasting-induced adipose factor FIAF, a novel peroxisome proliferator-activated receptor target gene. *J. Biol Chem.* **275**, 28488–28493 (2000).
- Ren, G., Kim, J. Y. & Smas, C. M. Identification of RIFL, a novel adipocyte-enriched insulin target gene with a role in lipid metabolism. *Am J Physiol Endocrinol Metab.* **303**, E334–E351 (2012).
- Ren, Z. Lipasin, a novel nutritionally-regulated liver-enriched factor that regulates serum triglyceride levels. *Biochem Biophys Res Commun.* **424**, 786–792 (2012).
- Lee, J. *et al.* AMP-activated protein kinase suppresses the expression of LXR/SREBP-1 signaling-induced ANGPTL8 in HepG2 cells. *Mol Cell Endocrinol.* **414**, 148–155 (2015).
- Nakajima, K. Remnant Lipoproteins: A Subfraction of Plasma Triglyceride-Rich Lipoproteins Associated with Postprandial Hyperlipidemia. *Clinical & Experimental Thrombosis and Hemostasis.* **1**, 45–53 (2014).
- Gusarova, V. *et al.* ANGPTL8/Betatrophin Does Not Control Pancreatic Beta Cell Expansion. *Cell.* **159**, 691–696 (2014).
- Bass, J. Circadian topology of metabolism. *Nature.* **491**, 348–356 (2012).
- Shimba, S. *et al.* Deficient of a clock gene, brain and muscle arnt-like protein-1 (BMAL1), induces dyslipidemia and ectopic fat formation. *PLoS One.* **6**, e25231 (2011).
- Sun, X. *et al.* Glucagon-CREB/CRTC2 signaling cascade regulates hepatic BMAL1 protein. *J. Biol Chem.* **290**, 2189–2197 (2015).
- Torra, I. P. *et al.* Circadian and glucocorticoid regulation of rev-erba expression in liver. *Endocrinology.* **141**, 3799–3806 (2000).
- Gallie, D. R. The cap and polyA tail function synergistically to regulate mRNA translational efficiency. *Genes Dev.* **5**, 2108–2116 (1991).
- Akashi, M. *et al.* Role of AUUU sequences in stabilization of granulocyte-macrophage colony stimulating factor RNA in stimulated cells. *Blood.* **78**, 2005–2012 (2005).

26. Vegiopoulos, A. & Herzig, S. Glucocorticoids, metabolism and metabolic diseases. *Mol Cell Endocrinol.* **275**, 43–61 (2007).
27. Woods, C. P., Hazlehurst, J. M. & Tomlinson, J. W. Glucocorticoids and non-alcoholic fatty liver disease. *J Steroid Biochem Mol Biol.* **154**, 94–103 (2015).
28. Steven, M. R. & David, R. W. Coordination of circadian timing in mammals. *Nature.* **418**, 935–941 (2002).
29. Dickmeis, T. Glucocorticoids and the circadian clock. *J. Endocrinol.* **200**, 3–22 (2009).
30. Lipton, J. O. *et al.* The Circadian Protein BMAL1 Regulates Translation in Response to S6K1-Mediated Phosphorylation. *Cell.* **161**, 1138–1151 (2015).
31. Cha, J. Y. & Repa, J. J. The liver X receptor (LXR) and hepatic lipogenesis. The carbohydrate-response element-binding protein is a target gene of LXR. *J. Biol Chem.* **282**, 743–751 (2007).
32. Kaplan, R. *et al.* Regulation of the angiopoietin-like protein 3 gene by LXR. *J. Lipid Res.* **44**, 136–143 (2002).
33. Ge, H. *et al.* Differential regulation and properties of angiopoietin-like proteins 3 and 4. *J. Lipid Res.* **46**, 1484–1490 (2005).
34. Koliwad, S. K. *et al.* Angiopoietin-like 4 (ANGPTL4, fasting-induced adipose factor) is a direct glucocorticoid receptor target and participates in glucocorticoid-regulated triglyceride metabolism. *J. Biol Chem.* **284**, 25593–25601 (2009).
35. Fu, Z., Abou-Samra, A. B. & Zhang, R. A lipasin/Angptl8 monoclonal antibody lowers mouse serum triglycerides involving increased postprandial activity of the cardiac lipoprotein lipase. *Sci Rep.* **5**, 18502, doi: 10.1038/srep18502 (2015).
36. Dijk, W. *et al.* ANGPTL4 mediates shuttling of lipid fuel to brown adipose tissue during sustained cold exposure. *eLife.* **4**, e08428, doi: 10.7554/eLife.08428 (2015).
37. Gray, N. E. *et al.* Angiopoietin-like 4 (Angptl4) protein is a physiological mediator of intracellular lipolysis in murine adipocytes. *J. Biol Chem.* **287**, 8444–8456 (2012).
38. Ren, Zhang. The ANGPTL3-4-8 model, a molecular mechanism for triglyceride trafficking. *Open Biol.* **6**, 150272, doi: 10.1098/rsob.150272 (2016).
39. Cong, L. *et al.* Multiplex Genome Engineering Using CRISPR/Cas Systems. *Science.* **339**, 819–823 (2013).
40. Luo, J. *et al.* A protocol for rapid generation of recombinant adenoviruses using the AdEasy system. *Nat Protoc.* **2**, 1236–1247 (2007).
41. Schmittgen, T. D. & Livak, K. J. Analyzing real-time PCR data by the comparative CT method. *Nat Protoc.* **3**, 1101–1108 (2008).
42. Patel, R. *et al.* LXR β is required for glucocorticoid-induced hyperglycemia and hepatosteatosis in mice. *J. Clin Invest.* **121**, 431–441 (2011).
43. Gao, Y. *et al.* Early adipogenesis is regulated through USP7-mediated deubiquitination of the histone acetyltransferase TIP60. *Nat. Commun.* **4**, 2656, doi: 10.1038/ncomms3656 (2013).

Acknowledgements

We thank Chenyao Wang (INS, SIBS, CAS, China) for the gift of px330 plasmid. This work was supported by grants from the National Natural Science Foundation of China (81390351), National Basic Research 973 Program (2014CB910500), NSFC (31471123 and 31222028), NBR973 (2012CB524900) and the Chinese Academy of Sciences (XDA12040306).

Author Contributions

F. D. and Y. L. conceived and designed the study. F. D. performed the experiments. R. W. helped perform experiments during revision. P. W., Md. S. A., Q. X. and Y. C. assisted with animal euthanization and sample collection. Y. W. assisted with adenovirus preparation. F. D. and Y. L. wrote the manuscript. Y. L. supervised the research.

Additional Information

Supplementary information accompanies this paper at <http://www.nature.com/srep>

Competing financial interests: The authors declare no competing financial interests.

How to cite this article: Dang, F. *et al.* Fasting and Feeding Signals Control the Oscillatory Expression of *Angptl8* to Modulate Lipid Metabolism. *Sci. Rep.* **6**, 36926; doi: 10.1038/srep36926 (2016).

Publisher's note: Springer Nature remains neutral with regard to jurisdictional claims in published maps and institutional affiliations.



This work is licensed under a Creative Commons Attribution 4.0 International License. The images or other third party material in this article are included in the article's Creative Commons license, unless indicated otherwise in the credit line; if the material is not included under the Creative Commons license, users will need to obtain permission from the license holder to reproduce the material. To view a copy of this license, visit <http://creativecommons.org/licenses/by/4.0/>

© The Author(s) 2016